# Optimizing ship manoeuvring time during port approach using a decision support system: A case study in Turkey

*Ender YALCIN[1*], Enes Fatih PEHLIVAN[2], Baris Anıl CETIN[3], Murat AYMELEK[4]*

[1]Department of Maritime Transportation and Management Engineering
Maritime Faculty, Bandirma Onyedi Eylul University, Balikesir, Turkey
eyalcin@bandirma.edu.tr

[2]Department of Naval Architecture and Marine Engineering
Marine Science Faculty, Ordu University, Ordu, Turkey
enespehlivan@odu.edu.tr

[3]Department of Maritime Transportation and Management,
Marine Science Faculty, Ordu University, Ordu, Turkey
bacetin@protonmail.com

[4]Department of Naval Architecture and Marine Engineering, Barbaros Hayrettin Naval Architecture and Maritime Faculty, Iskenderun Technical University, Hatay, Turkey.
murat.aymelek@iste.edu.tr

* Corresponding author. Tel: +90 542 484 2004

## ABSTRACT

Currently, in practice, ship captains are responsible for decision-making during the manoeuvring process. However, this could be improved upon by the assistance of a decision support system. Any cost reductive initiative is significant to contribute to the overall viability and economic sustainability of the industry. Therefore, it is worthy to study time and cost efficiency of ship manoeuvring when approaching the port. This study develops a decision support system model by utilizing a goal programming integrated ship manoeuvring methodology, which examines ship and environmental variables concerning manoeuvring. The methodology enables positive resultant force of the ship and tugboat against negative external parameters with minimum effort and time. A case study was then carried out using 2 different container ships approaching Gemport berths in Turkey, to show the practical applicability of the methodology. The results of the case study showed that it would be possible to reduce manoeuvring time in approaching the port from 31.6 minutes to 27.36 minutes in ship I and from 59 minutes to 48.05 minutes in ship II. These results are significant as they can provide cost efficiency for ship owners and port authorities, especially when we consider its applicability for the entire world merchant marine fleet.

**Keywords:** Ship manoeuvring, port approach, decision support, goal programming

## 1. Introduction

Ship manoeuvring is a time-consuming aspect of port operations in the maritime transport industry. However, managing ships manoeuvring time is a complex task. In fact, it is an operational outcome from a number of events occurring in manoeuvring process as a repercussion of the actions taken by the ships' watch-keeping crew (Fan et al. 2018). Nevertheless, a bridge team of a ship faces complex decisions regarding manoeuvring consisting of many parameters, while approaching the port quay. These decisions include management of the ships' own resources and propulsion systems, as well as towage and pilotage services available in the port area. Additionally, ship and external environment variables of manoeuvring are also taken into consideration when approaching the port. All of these combined factors have an essential influence on the general operational efficiency and time management of ships in the port area (Ugurlu et al. 2014; Tilling and Ringsberg, 2019; Zinchenko et al. 2022).

Since the 2008 global economic crisis affected the shipping industry, the negative outcomes can be noticed financially (Shin et al. 2019). Therefore, internal resource-based views gained vital importance in the effective management of shipping companies. This includes operational efficiency, as well as administrative cost efficiency of shipping companies in order to remain competitive (Wang et al. 2020). The ships' time spent in port is one of the major contributing cost elements to the balance sheet of ship owners today (Zheng et al. 2022). Thus, any initiative aiming to reduce port time can have a positive effect on the financial stability of the industry. These reasons catch attention of researchers. In this article, a rigorous literature review was carried out in order to scrutinize previous studies and determine the research gap. The findings from the literature showed that many studies such as Feng et al. (2020) and Moon and Woo (2014), have previously been carried out which discuss the effect of the ship's time in port, however little has been done specifically on optimizing ship manoeuvring time in port.

The main purpose of the research is optimizing ship's time spent in port by developing a decision support system tool to enhance manoeuvring decision-making process. Usage of this system would not only reduce the workload of crew but would also provide cost efficiency. In order to establish this necessary decision support tool, a goal programming methodology has been applied. Testing the methodology in practice, the case study has been carried out. For the case study, data were collected from the two container ships operating in Turkish port and an analysis was carried out to attain the results. Optimization during the manoeuvre time was pursued, from which point and with what force tug support was provided during the manoeuvring of a ship (Lu et al. 2019).

Within the scope of the study, the components of ship hydrodynamics and environmental dynamics are scrutinized by referring to mathematical models. Particularly the effectiveness of manoeuvring decisions when employing a tugboat are measured by calculating the total manoeuvring time periods of the ship, as well as taking safety procedures into account. Additionally, by applying the system, time optimization is supposed to be achieved by ship port docking manoeuvres and safety risks arising from ships are minimized. The remaining part of the paper consists of literature review, hydrodynamic forces through ship manoeuvring, proposed methodology, case study, results and discussion, and conclusion.

## 2. Literature Review

Ship manoeuvring topic draw attention in the literature contemporary due to its significance for shipping company economics. Broadly, ship manoeuvring decisions are complex decision-making concepts which include many internal and external variables (Xue et al. 2019). The dimensions of the ship, engine types, type of propellers can be given as examples of internal variables. Besides, wind and tidal effects, weather conditions, depth of water are basic examples of external variables which play an important role in ship manoeuvring. Manoeuvring and berthing operations have many decision criteria in terms of available port superstructure and infrastructure, and also have many controllable and uncontrollable variables in the decision-making process (Nakamura, 2017). Therefore, to concentrate on controllable variables is more suitable to generate minimum port operation time for ship manoeuvring decision-making.

One of the main reasons to focus to the shipping industry is cost efficiency and operational productivity (Moon and Woo 2014). The main aim of focusing on efficiency is minimisation of the total time spent for port operations, including manoeuvring and berthing. Several studies stressed it by manoeuvring time and some parameters such as wind-wave-current conditions (Bai et al. 2018) and hull features (Wang et al. 2017). Although in terms of economic efficiency, even a little time reduction is very important for shipowners, cargo owners and port/terminal operators. Therefore, an improvement in the manoeuvring period will mean that a significant amount of money can be saved not only for ship owners and cargo owners but also for port or terminal operators (Shahpanah et al. 2014).

The optimization of ship manoeuvring to avoid ship accidents and the effect of human factor on these accidents are one of the main trends in the literature. For instance, Zhang et al. (2017) developed a simulation model to improve manoeuvring safety by dividing ship motion into two parts including low frequency manoeuvring part and high frequency seakeeping part. In another study, in order to improve manoeuvring safety, Yasukawa and Yoshimura (2015)

proposed a manoeuvring modelling group standard method consisting of four aspects namely the manoeuvring simulation model, the procedure of the required captive model tests, the analysis method, and the prediction method. Ship manoeuvring safety in shallow and confined water was also scrutinized by Vantorre et al. (2017) and Xu et al.(2017). Similarly, Budak and Beji (2020) also studied narrow waterways ship manoeuvring in the Bosporus Strait by using a numerical simulation which compared the human involvement and automation in ship manoeuvring process. Furthermore, a systematic literature review has been conducted to reveal relationship decisions support and ship accident by considering several categories such as collision avoidance, ship manoeuvring, weather conditions etc. (Gil et al. 2020). According to these categories, the authors reported the role and aim of decision support system as "*calculating and proposing an evasive manoeuvre, automatic or supported execution of vessel manoeuvres, improvement of ship motions in various operational conditions, improvement and optimization of voyage parameters caused by hydrometeorological conditions, estimation of the impact of wind or waves on ship hull*".

In related study, Bai et al. (2018) conducted series of trials in ship manoeuvring system by applying multi-innovation gradient iterative algorithm. In another study, Seo and Kim (2011) applied numerical methods to analyse ship manoeuvring time for defining two problems, space-fixed and ship-fixed coordinate systems. Computational fluid dynamic calculations are also used to predict ship manoeuvring time by Liu et al. (2018). This methodology is also applied to scrutinize hydrodynamic effects and analyze responses (Du et al. 2021). One of the most popular machine learning methodologies, support vector machine is used to diagnose parameters in ship manoeuvring by Wang et al. (2021). Time domain software, like ELIGMOS, is applied to manoeuvring of ship modelling in regular waves (Pollalis et al. 2021). Neri (2018) and Alexandersson et al. (2022) conducted a research regarding ship motion simulation and provided a ship manoeuvring prediction by applying a time-domain algorithm. Another study about manoeuvring in regular waves was modelled for container ships by Rameesha and Krishnankutty (2018). They concluded that even in designing of ships wave characteristics should be taken into account. It is obvious that there are many different methodologies attempting to model and predict ship manoeuvring and there are different aims by applying these methods. However, none of these studies encompasses a goal programming methodology in order to develop a decision support system to enhance manoeuvring time in port.

The ship manoeuvring decision support system based on goal programming maybe not only provide time efficiency but also may prevent collision risks in ports. There are many collision risks such as ship berthing crashes in a pier (Hsu 2015, Kuzu et al. 2019). These kinds

of collisions not only have economic consequences but also negative social and environmental impacts (Luo et al. 2017). It is clear that even though the absence of support decision systems is not the primary contributing factor for accidents, the system has a crucial role to prevent collisions in manoeuvring. Based on the ship manoeuvring technical background, the methodology of this study presents a practical framework of goal programming integrated ship manoeuvring during port approach which contributes to time, cost and environmental efficiency as well as safety of manoeuvring operations. The methodology is also applied on a case study to obtain numerical results from the actual practice as summarised in Fig. 1.

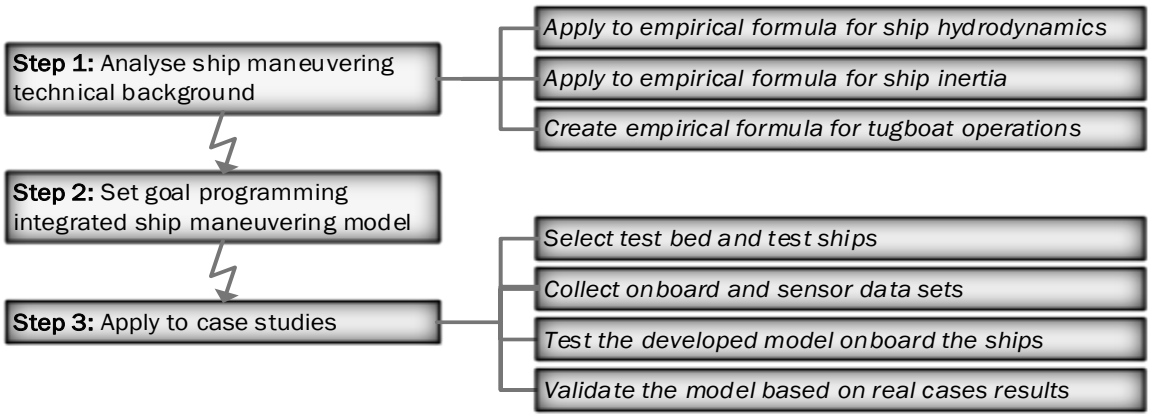


**Figure 1.** Workflow of the research.

## 3. Proposed Methodology

### *3.1. Goal Programming*

Linear programming models have been used in the past to investigate a wide-range of issues in various sectors. They are the traditional ways of analysing different quantitative parameters. However, there are certain problems with the use of linear programming in real industry practice. One of these is that there is a single objective in this kind of model San Cristóbal (2012b) and it is possible to be faced with an unmitigated hard row to hoe in the case of having more than one objective. In 1957, Charnes and Cooper (1957) formulated a goal programming (GP) theory which is a special form of linear programming (Leung and Ng 2007), and a new and convenient synthetic procedure to assess more than one objective (Aouni and Kettani 2001) draw our attention to distinctive extensions of GP and also found that weighted GP is one of the most popular ways among these extensions.

According to Romero (2004), a key component of GP is the achievement function that speaks to a numerical expression of the undesirable deviation factors from a reference point of the sequence of events. In the weighted GP (WGP), the achievement function encompasses all unwanted deviation variables (udv) and each deviation variables are weighted expediently on

their importance level. The WGP has been formulized by Ignizio (1976) and Romero (2004) as below:

$$Min\sum_{i=1}^{q}(\alpha_i n_i + \beta_i p_i) \tag{16}$$

where the goals and constraints are

$$f_i(x) + n_i - p_i = t_i, i \in \{1,...,q\}, x \in F, n \geq 0, p \geq 0$$

$t_i$ is target level for the *i*th goal,

$n_i$, $p_i$ are negative and positive deviations from target value of *i*th goal,

x is vector of decision variables,

F is attainable set of constraints,

$\alpha_i = w_i / k_i$ where $n_i$ is udv. If there is no udv, it equals to 0.

$\beta_i = w_i / k_i$ where $p_i$ is udv. If there is no udv, it equals to 0.

$w_i$ and $k_i$ are illustrative weights of importance level.

*3.2. Goal Programming Integrated Ship Manoeuvring Model*

The propelling and total resistance forces (see Appendix II) can play an important role in addressing the issue of ship manoeuvring. The propelling force depends on ship service speed, and service speed is controlled by ship telegraph commands. Since a ship engaged voyage in a straight line, it might be said that the service speed, which is changeable with different telegraph commands such as full ahead (FAh), half ahead (HAh), slow ahead (SAh), dead slow ahead (DSAh), stop engine (SE), dead slow astern (DSa), slow astern (Sa), half astern (Ha) and full astern (Fa), express a driving force for the ship in consideration of current, wave and wind forces in the marine environment. Throughout the port approach, a ship follows a specific route which includes route legs from the pilot embarkation point to berth at which the course is changed to ensure safe navigation. The each of route legs is displayed as a straight line which defines the shortest route between two consecutive waypoints to enable safety navigation by considering safety distance, turn-radius constraints and safety depth-contour in the presence of movable or stationary obstacles (Ari et al. 2013). The ships change their course frequently between two route legs and in such a case, helm order or rudder angle causes vectorial components of speed that could be measured with $\sin\theta$ for x axis and $\cos\theta$ for y axis where $\theta$ means an angle between x axis and new ship course after rudder command where reference system for x and y is earth bound.

The helm orders and telegraph commands lead to produce a force with the contribution of resistance forces in reverse direction. This force refers to a net manoeuvring force, which indicates final movement tendency under different environmental parameters and ship inertia. In this force, vectorial components (e.g., transverse and longitudinal) of distance covered (mile/knot) will be used to describe this phenomenon respectively, in x (dx) and y axis (dy).

$$dx = \left[\left(c_{FAh} - r_{FAh}\right)\cdot\cos\theta \pm \left(c_{Cur}\cdot\cos\beta\right)\right]\cdot t_{FAh} + \left[\left(c_{HAh} - r_{HAh}\right)\cdot\cos\theta \pm \left(c_{Cur}\cdot\cos\beta\right)\right]\cdot t_{HAh} + \left[\left(c_{SAh} - r_{SAh}\right)\cdot\cos\theta \pm \left(c_{Cur}\cdot\cos\beta\right)\right]\cdot t_{SAh} + \left[\left(c_{DSAh} - r_{DSAh}\right)\cdot\cos\theta \pm \left(c_{Cur}\cdot\cos\beta\right)\right]\cdot t_{DSAh} - \left[\left(c_{DSa} - r_{DSa}\right)\cdot\cos\theta \pm \left(c_{Cur}\cdot\cos\beta\right)\right]\cdot t_{DSa} - \left[\left(c_{Sa} - r_{Sa}\right)\cdot\cos\theta \pm \left(c_{Cur}\cdot\cos\beta\right)\right]\cdot t_{Sa} - \left[\left(c_{Ha} - r_{Ha}\right)\cdot\cos\theta \pm \left(c_{Cur}\cdot\cos\beta\right)\right]\cdot t_{Ha} - \left[\left(c_{Fa} - r_{Fa}\right)\cdot\cos\theta \pm \left(c_{Cur}\cdot\cos\beta\right)\right]\cdot t_{Fa} + \Delta S_{DSAh\to 0}\cdot\cos\theta + c_{Tx}t_{Tx} \quad (186)$$

$$dy = \left[\left(c_{FAh} - r_{FAh}\right)\cdot\sin\theta \pm \left(c_{Cur}\cdot\sin\beta\right)\right]\cdot t_{FAh} + \left[\left(c_{HAh} - r_{HAh}\right)\cdot\sin\theta \pm \left(c_{Cur}\cdot\sin\beta\right)\right]\cdot t_{HAh} + \left[\left(c_{HAh} - r_{HAh}\right)\cdot\sin\theta \pm \left(c_{Cur}\cdot\sin\beta\right)\right]\cdot t_{HAh} + \left[\left(c_{SAh} - r_{SAh}\right)\cdot\sin\theta \pm \left(c_{Cur}\cdot\sin\beta\right)\right]\cdot t_{SAh} + \left[\left(c_{DSAh} - r_{DSAh}\right)\cdot\sin\theta \pm \left(c_{Cur}\cdot\sin\beta\right)\right]\cdot t_{DSAh} - \left[\left(c_{DSa} - r_{DSa}\right)\cdot\sin\theta \pm \left(c_{Cur}\cdot\sin\beta\right)\right]\cdot t_{DSa} - \left[\left(c_{Sa} - r_{Sa}\right)\cdot\sin\theta \pm \left(c_{Cur}\cdot\sin\beta\right)\right]\cdot t_{Sa} - \left[\left(c_{Ha} - r_{Ha}\right)\cdot\sin\theta \pm \left(c_{Cur}\cdot\sin\beta\right)\right]\cdot t_{Ha} - \left[\left(c_{Fa} - r_{Fa}\right)\cdot\sin\theta \pm \left(c_{Cur}\cdot\sin\beta\right)\right]\cdot t_{Fa} + \Delta S_{DSAh\to 0}\cdot\sin\theta + c_{Ty}t_{Ty} \quad (187)$$

In here,

c values ($c_{FAh}, c_{HAh}, c_{SAh}, c_{DSAh}, c_{DSa}, c_{Sa}, c_{Ha}, c_{Fa}$) are the speed coefficients for each telegraph commands,

$c_{Cur}$ is the current speed,

$c_{Tx}$ is the speed coefficient for tugboat operations in x direction,

$c_{Ty}$ is the speed coefficient for tugboat operations in y direction.

r values ($r_{FAh}, r_{HAh}, r_{SAh}, r_{DSAh}, r_{DSa}, r_{Sa}, r_{Ha}, r_{Fa}$) are the resistance force coefficients for each telegraph commands,

$t_i$ is time value where $i$ is passing time in each telegraph command and $i \in (t_{FAh}, t_{HAh}, t_{SAh}, t_{DSAh}, t_{DSa}, t_{Sa}, t_{Ha}, t_{Fa})$,

$t_{Tx}$ is tugboat (s) operation time in x axis,

$t_{Ty}$ is tugboat (s) operation time in y axis,

$t_T$ is total tugboat operation time,

$\beta$ is an angle between current vector and x axis, and $\theta$ is an angle that can be calculated with subtraction target course in each route leg.

Therefore, an achievement function for GPISM model is written as below:

Minimize $t_{FAh} + t_{HAh} + t_{SAh} + t_{DSAh} + t_{DSa} + t_{Sa} + t_{Ha} + t_{Fa} + \Delta t_{DSAh\to 0} + t_T$ (17)

Goal $t_{FAh} + t_{HAh} + t_{SAh} + t_{DSAh} + \Delta t_{DSAh\to 0} + t_T \le t_{AVG}$

Constraints

1. If $[(c_{FAh} - r_{FAh}).\cos\theta \pm (c_{Cur}.\cos\beta)].t_{FAh} + \Delta S_{DSAh\to 0}.\cos\theta \pm c_{Tx}t_{Tx} \ge dx, t_{FAh} = 0$

2. If $[(c_{FAh} - r_{FAh}).\cos\theta \pm (c_{Cur}.\cos\beta)].t_{FAh} + \Delta S_{DSAh\to 0}.\cos\theta \pm c_{Tx}t_{Tx} \le dx,$
$t_{HAh} + t_{SAh} + t_{DSAh} = 0$

$$t_{FAh} = \frac{dy - \Delta S_{DSAh\to 0}.\sin\theta - c_{Tx}.t_{Tx}}{(c_{FAh} - r_{FAh}).\sin\theta \pm (c_{Cur}.\sin\beta)}$$

3. If $[(c_{HAh} - r_{HAh}).\cos\theta \pm (c_{Cur}.\cos\beta)].t_{HAh} + \Delta S_{DSAh\to 0}.\cos\theta \pm c_{Tx}t_{Tx} \le dx$
$and, [(c_{FAh} - r_{FAh}).\cos\theta \pm (c_{Cur}.\cos\beta)].t_{FAh} + \Delta S_{DSAh\to 0}.\cos\theta \pm c_{Tx}t_{Tx} \ge dx,$
$t_{FAh} + t_{SAh} + t_{DSAh} = 0$

$$t_{HAh} = \frac{dy - \Delta S_{DSAh\to 0}.\sin\theta - c_{Tx}.t_{Tx}}{(c_{HAh} - r_{HAh}).\sin\theta \pm (c_{Cur}.\sin\beta)}$$

4. If $[(c_{SAh} - r_{SAh}).\cos\theta \pm (c_{Cur}.\cos\beta)].t_{SAh} + \Delta S_{DSAh\to 0}.\cos\theta \pm c_{Tx}t_{Tx} \le dx$
$and, [(c_{HAh} - r_{HAh}).\cos\theta \pm (c_{Cur}.\cos\beta)].t_{HAh} + \Delta S_{DSAh\to 0}.\cos\theta \pm c_{Tx}t_{Tx} \ge dx,$
$t_{FAh} + t_{HAh} + t_{DSAh} = 0$

$$t_{SAh} = \frac{dy - \Delta S_{DSAh\to 0}.\sin\theta - c_{Tx}.t_{Tx}}{(c_{SAh} - r_{SAh}).\sin\theta \pm (c_{Cur}.\sin\beta)}$$

5. If $[(c_{DSAh} - r_{DSAh}).\cos\theta \pm (c_{Cur}.\cos\beta)].t_{DSAh} + \Delta S_{DSAh\to 0}.\cos\theta \pm c_{Tx}t_{Tx} \le dx$
$and, [(c_{SAh} - r_{SAh}).\cos\theta \pm (c_{Cur}.\cos\beta)].t_{SAh} + \Delta S_{DSAh\to 0}.\cos\theta \pm c_{Tx}t_{Tx} \ge dx,$
$t_{FAh} + t_{HAh} + t_{SAh} = 0$

$$t_{DSAh} = \frac{dy - \Delta S_{DSAh\to 0}.\sin\theta - c_{Tx}.t_{Tx}}{(c_{DSAh} - r_{DSAh}).\sin\theta \pm (c_{Cur}.\sin\beta)}$$

$\Delta t_{DSAh\to 0} = t_{DSAh} - t_0$, where $\Delta t$ is the passing time until ship inertia is zero ( $t_0$ ) after stop engine telegraph command.

$$t_T = t_{Tx} + t_{Ty}, where \begin{cases} for\_pulling\_t_{Tx} = \dfrac{m(V - V_{0x})}{F_T - F_{Rx}} + \dfrac{m}{k_3.\upsilon_{Sk_3}}\left[\arctan\dfrac{V_{0x}}{\upsilon_{Sk_3}} - \arctan\dfrac{V}{\upsilon_{Sk_3}}\right], \\ otherwise\_t_{Tx} = 0 \\ for\_pushing\_t_{Ty} = \dfrac{m(V - V_{0y})}{F_T - F_{Ry}} + \dfrac{m}{k_3.\upsilon_{Sk_3}}\left[\arctan\dfrac{V_{0x}}{\upsilon_{Sk_3}} - \arctan\dfrac{V}{\upsilon_{Sk_3}}\right], \\ otherwise\_t_{Ty} = 0 \end{cases}$$

A primary concern of the achievement function is to save total maneuvering time and prevent any possible safety risk during ship maneuvering. For this reason, the goal has been set to the best value which is less than average maneuvering time ($t_{AVG}$) according to previously recorded maneuvering facts. Total maneuvering time is dependent on two contributing factors including total travelled distance and ship speed. To reduce total maneuvering time, the basic rules are to minimize total travelled distance and maximize ship speed throughout the maneuvering process. To minimize total travelled distance, ship motion in the y-axis ($dy$) has to be reduced to the minimum value and ship motion in the x-axis ($dx$) has to be increased to the maximum value. However, travelled distance under the effect of different telegraph commands cannot be greater than $dx$ due to the ship speed related safety issues such as collision to berth or other ships. To maximize ship speed, the most appropriate telegraph command, which leads to higher ship speed, has been applied into the practice. The stopping distance of the ship under the different telegraph commands has been considered in this process. Similar to shipping practice, five different scenarios have been defined based on stopping distance for each telegraph command by considering the produced forces by ship engines including ship resistance, ship inertia, and the produced force by tugboat to define constraints in the achievement function. In the first constraint (scenario), the ship engages in voyage with full speed within a certain time ($((c_{FAh} - r_{FAh}).\cos\theta \pm (c_{Cur}.\cos\beta)].t_{FAh}$) and when the ship engines were stopped and tugboat(s) are used, travelled distance in x-axis due to the ship inertia and tugboat pulling is computed with the equation $\Delta S_{DSAh\to 0}.\cos\theta \pm c_{Tx}t_{Tx}$. If the multiplication of these two equations is greater than the dx value, a lower speed value is used instead of full speed command in the second scenario due to the safety issues. The same procedure is followed when computed value was greater than the dx value of total travelled distance within the third, fourth and finally fifth scenarios.

## 4. Case Study

Once the modelling of ship manoeuvring environment in port approach through different ship and environmental parameters was completed, it was necessary to model validation test(s) to determine the acceptability and usability of the model in the real world. In this paper, the validation was carried out in two different case studies by conducting a validation process with real world manoeuvring data sets and experts which include ocean-going master, watch-keeping officer(s), engineer(s) of a selected ship and master of a tugboat.

*4.1. Selection of Test Bed and Test Ship(s)*

The test bed has been selected for two case studies from Gemport port, Gulf of Gemlik in Turkey. Gemport is called as an open roadstead and fairly shelter afforded harbour by natural structure of Gulf of Gemlik with zero tide (URL-1, 2022). Sea state in the region is frequently calm and severe sea conditions such as very rough, high, very high are not much observed due to limited fetch area (Altunc et al. 2013). The Gemport port has 13 berths (see Fig. 3) and 6 deep-sea tugs to help manoeuvring within the port region and between the berths (Cetin 2020).


**Figure 3.** General arrangement plan of Gemport (URL-2, 2021).

Due to permission requirements to collect on board data, available and accessible two ships, which called the Gemport port, have been selected to apply onboard test activities. The fundamental information about ships is summarised as Appendix III in line with the data confidentialities of the ship owner companies as well as Appendix IV.

*4.2. Data Collection*

After the selection of test bed and test ships, particular data collection procedures have been followed in compliance with the case study requirements. Additionally, the authors conducted a series of operational observations in the data collection processes including:

i) recording of commands and command times which are given by the master and pilot onboard of the test ship,

ii) recording the actions and times of the tugboat and ship engines by contribution of the commands of tugboat master and ship engineer(s),

iii) receiving the ship automatic identification system (AIS) and sensor data to reveal the speed coefficients as given in Appendix V and VI, which refer to average speed values, and are calculated by comparing different telegraph commands under the impact of environmental instruments and ship's technical capabilities,

iv) meteorological data in the selected area,

v) the selected ship's technical information.

In this process, the AIS and meteorological data sets have been obtained via ship and tugboat sensors and ship crews have provided the ship's technical information.

## 5. Results and Discussion

The real time ship manoeuvring on-board is a reliable and appropriate method when all parameters in port approach manoeuvring are considered. For this reason, in this study, two real time ship manoeuvring were used. The proposed model suggestions have been applied into the ship manoeuvring operation of two ships in Gemport port approaching. Ultimately, the results were compared with the previously recorded ship tracking data (see, Fig. 4), followed route for two cases, which indicate a difference of 4.95% for Ship I and 16% for Ship II. The major alteration in here is caused by deviated cruising of ships due to the external environmental conditions. However, those conditions are not considered as threats to the navigational safety. Within these limitations, the findings of this study validated that the chosen route was appropriate for the selected case studies.

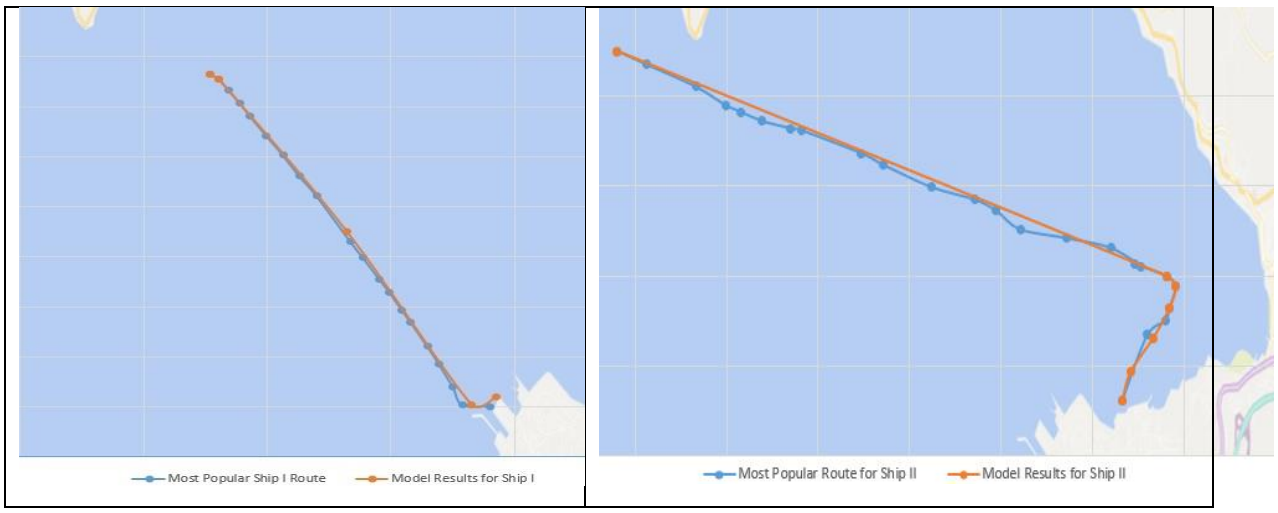


**Figure 4.** Comparisons of the AIS-data based most popular routes (blue colours) for Ship I (left) and Ship II (right) with the model results (orange colours).

Several ship accidents have shown that the selection of proper ship speed is crucial for safe navigation in port approach, and there is a strong relationship between ship speed selection and remaining distance (Kang et al. 2019). It is interesting to note that in both case studies, it is almost certain that a ship accident occurs as a result of high speed under full ahead telegraph command from pilot position to berthing. Another interesting practical inference emerged from the analysis is that appropriate telegraph command is limited to half ahead which causes

maximum ship speed to avoid risky situations. These are also confirmed with the onboard manoeuvring trial results which are given in Appendix VII.

Current force-direction and wind force-direction are a common condition which have considerable impact on ship manoeuvring as well as selection of ship speed (Fan et al. 2020). Current was observed in the range of 0.68 and 0.77 knots, and north-north east direction for the test bed in the data collection period. While wind was observed average 8 knots in 201° directions and sea state was calm for Ship I, they are also 227° directions and calm for Ship II maneuvering period. The authors paid particular attention to prevailing waveform in selected day of test-bed is the regular wave suitable for Holtrop-Mennen method. The findings obtained from the preliminary analysis of ship speed co-efficient for selected ships were presented by considering ship propeller force and ship interaction, current force-directions and wind force-directions in each telegraph commands in Table 2.

**Table 2.** Ship speed co-efficient for each telegraph commands.

| Variable | Ship I | Ship II |
|---|---|---|
| DSAh | 2.4 | 2.38 |
| Sah | 3.985 | 4.96 |
| Hah | 5.84 | 7.58 |
| FAh | 8.6 | 12.6 |

Based on previous port manoeuvring experiences, the average total passing time from the pilot embarkation point or anchor position to waiting in position for mooring was found for Ship I and Ship II respectively, 31.6 and 59 minutes, and average of distance covered was found for Ship I and Ship II respectively as 1.5494 and 3.321 miles in test bed.

With respect to the numerical analysis of ship acceleration or deceleration, it was found that there is a long-time ( $\Delta t$ ) and enough distance ( $\Delta s$ ) requirement for the transition from one variable to another which is defined in Table 3. These time requirements describe the relationship between ship mass, environmental parameters and amount of force to continuously accelerate or decelerate the ship in case of movement by the ships' own means. However, it is possible to reduce the manoeuvring time with the contribution of additional pushing and/or pulling forces according to Newton's second law. In the port approaching practice, these forces are provided by tugs. In previous studies such as Hansen (2020) the authors evaluated tug requirements as per ship mass and environmental parameters in the manoeuvring area. The reported tug bollard pull was 411.80 kN for Ship I and 441.30 kN for Ship II, and required tug number was 1 for Ship I and 2 for Ship II according to these parameters.

**Table 3.** Numerical analysis of ship acceleration from DSAh to HAh and ship deceleration from HAh to SE for onboard cases.

| Variable | Ship I | | | | Ship II | | | |
|---|---|---|---|---|---|---|---|---|
| | $R_T$ (kN) | Ship Inertia (kN) | $\Delta s$ * (miles) | $\Delta t$ ** (min) | $R_T$ (kN) | Ship Inertia (kN) | $\Delta s$ (miles) | $\Delta t$ (min) |
| $DSAh \rightarrow HAh$ | 14.69 | 16.16 | 0.40 | 10.4 | 21.79 | 22.88 | 0.62 | 19.44 |
| $HAh \rightarrow DSAh$ | 79.32 | 87.25 | 0.27 | 9.34 | 79.32 | 87.25 | 3.21 | 36 |
| $DSAh \rightarrow SE$ | 14.69 | 16.16 | 0.89 | 47.98 | 14.69 | 16.16 | 1.29 | 50.85 |

* $\Delta s$ is the required distance (miles) to shift from one telegraph command to another.

** $\Delta t$ is the required time (minutes) to shift from one telegraph command to another.

On the question of how the tug reduces the required time for manoeuvring during the period of DSAh command to SE, this study found that it is likely to cut down on passing time to 10.27 minutes for Ship I and 0.13 minutes for Ship II based on recommended model and total force interaction (see breakdown of hydrodynamic forces for each ship in Appendix VIII). The main reason of this difference in two different case studies is the more frequent change of course during port approach. Since change of course for the ship occurred due to ship route necessity or obstacles in the ship route, the ship speed decreases depending on the angle of rotation for the new route even if the ship proceed with constant engine power. Therefore, course alteration in ships have also been considered in the case studies as well as the contribution of tugs, and all desired events in port approach could be summarized with the contribution of tug pushing and pulling action and ship manoeuvring facts, as in Table 4.

**Table 4.** The breakdown of manoeuvring parameters during the ships' port approaching.

| Ship I | | | | | Ship II | | | | |
|---|---|---|---|---|---|---|---|---|---|
| Leg ID | COG (°) | SOG (knot) | x axis (m) | y axis (m) | Leg ID | COG (°) | SOG (knot) | x axis (m) | y axis (m) |
| Leg _1 | 172 | 4.075 | 945.5 | 311.8 | Leg _1 | 90 | 2.38 | 1152 | - |
| Leg _1 | 172 | 5.84 | 1261 | 588.36 | Leg _1 | 90 | 7.58 | 4155 | - |
| Leg _2 | 142 | 4.87 | 904 | 600.65 | Leg _1 | 90 | 4.97 | 5935.5 | - |
| Leg _3 | 122 | 2.38 | 1000 | 6258 | Leg _2 | 110 | 4.17 | 0.189 | 1.21 |
| | | | | | Leg _3 | 120 | 2.03 | 0.253 | 0.57 |
| | | | | | Leg _4 | 150 | 0.77 | 1.005 | 0.32 |
| | | | | | Leg _5 | 120 | 0.77 | 0.109 | 0.70 |
| | | | | | Leg _6 | 90 | 0.77 | 0.095 | 0.61 |
| | | | | | Leg _7 | 80 | 2.38 | 0.163 | 2.99 |
| | | | | | Leg _7 | 80 | 4.17 | 0.101 | 0.07 |
| Pushing Time (min.) | | | | 10.27 | Pushing Time (min.) | | | | 9.55 |
| Pulling Time (min.) | | | | 0.82 | Pulling Time (min.) | | | | 0.13 |

## 6. Conclusion

In this study, a model for decision making in port approach and manoeuvring has been presented. The model integrates goal programming and mathematical models of ship motion which identifies dynamic and static parameters effecting the total manoeuvring time. The developed goal programming integrated ship manoeuvring model has been validated in a case study for two ships. The findings of this analysis were compared with previous experiences and therefore, two broad themes emerged from the analysis. Firstly, there was a correlation with the total manoeuvring time and course alteration frequency because the ship speed decreases rapidly as long as the ship course changes. The minimum number of route legs, which will lead to safe navigation and the shortest route between the starting point of the intended voyage and destination, is the first rule of manoeuvring. Secondly, since a ship telegraph was changed from dead slow ahead to stop engine, a full stop of the ship would have taken a long time by the effect of ship inertia. However, this time period was reduced from 47.98 minutes to 0.82 minutes for Ship I, from 50.85 minutes to 0.13 minutes for Ship II by the contribution of effective tugboat pulling operation in reverse direction to ship inertia. Therefore, one could see that the timely and effective tugboat planning in manoeuvring is the second rule of manoeuvring. In practice, the use of the two aforementioned rules at the same time, reduced the total manoeuvring time to 27.36 minutes in Ship I, 48.05 minutes in Ship II. Together these results provide important insights into port manoeuvring related decision-making processes and overall, these results indicate that goal programming integrated maneuvering model provides some support for the conceptual framework of effective ship manoeuvring in port approach since the results were compared with previous manoeuvring experiences such as average 31.6 minutes for Ship I and 59 minutes for Ship II and with test results respectively 27.36 and 48.05 minutes. The results of this study also have important implications for developing novel risk assessment and management strategies. In future investigations, it might be possible to use this model in order to evaluate dynamic risk assessment approaches.

## Acknowledgements

The authors would like to thank Yılport Holding for data collection permission both onboard and tugboat(s). The authors also thank the oceangoing master, watchkeeping officer(s), engineer(s) of the case study ships, master of the tugboat(s) and academics which made a big contribution to onboard validation process.

## References


Abel-Günther K, Keil H. 1994. Handbuch Der Werften 22: Schiffahrts-Verlag Hansa.

Alexandersson M, Zhang D., Mao W., Rinsgberg. J. B. 2022. A comparison of ship manoeuvrability models to approximate ship navigation trajectories. Ships and Offshore Structures, 1-8.

Altunc M, Yilmaz A, Yalcin E. Bodrum Sahilleri ve Cevresinde Dalga Analizi. Proceedings of the 5th National Maritime Conference; 2013 11th December: Poster Presentation.

Aouni Bd, Kettani O. 2001. Goal programming model: A glorious history and a promising future. European Journal of Operational Research.133:225-231.

Ari I, Aksakalli V, Aydogdu V, Kum S. 2013. Optimal ship navigation with safety distance and realistic turn constraints. European Journal of Operational Research.229:707-717.

Bai W-w, Ren J-s, Li T-s. 2018. Multi-Innovation Gradient Iterative Locally Weighted Learning Identification for A Nonlinear Ship Maneuvering System. China Ocean Engineering. 2018/06/01;32:288-300.

Bertram V. 2012. Practical Ship Hydrodynamics. Second ed. Butterworth-Heinemann: Elsevier.

Bertram V, Wobig M. 1999. Simple empirical formula to estimate main form parameters of ships. Schiff and Hafen.11:118–121.

Birk L. 2019. Fundamentals of Ship Hydrodynamics Fluid Mechanics, Ship Resistance and Propulsion United Kingdom: John Wiley and Sons.

Budak G, Beji S. 2020. Controlled course-keeping simulations of a ship under external disturbances. Ocean Engineering. 2020/12/15/;218:108126.

Cetin BA. 2020. Gemport Port. In.

Charnes A, Cooper WW. 1957. Management Models and Industrial Applications of Linear Programming. Management Science.4:38-91.

Du Y, Zheng M, Liang X, Wang Y, Chai Z, Jo H, Duan M. 2021. Experimental and numerical investigation of hydrodynamic coefficients of subsea manifolds. Ships and Offshore Structures.16:595-607.

Fan S, Zhang J, Blanco-Davis E, Yang Z, Wang J, Yan X. 2018. Effects of seafarers' emotion on human performance using bridge simulation. Ocean Engineering. 2018/12/15/;170:111-119.

Feng M, Shaw S-L, Peng G, Fang Z. 2020. Time efficiency assessment of ship movements in maritime ports: A case study of two ports based on AIS data. Journal of Transport Geography. 2020/06/01/;86:102741.

Gil M, Wróbel K, Montewka J, Goerlandt F. 2020. A bibliometric analysis and systematic review of shipboard Decision Support Systems for accident prevention. Safety Science. 2020/08/01/;128:104717.

Guldhammer HE, Harvald SA. 1974. Ship resistance : effect of form and principal dimensions (Revised) Copenhagen: Akademisk Forlag.

DNV Towing Requirements. Available from http://www.tugmasters.org/wp-content/uploads/2014/07/Towingrecomends.pdf

Holtrop J. 1977. A Statistical Analysis of Performance Test Results. IS Progress.

Holtrop J. 1984. A Statistical Re-Analysis of Resistance and Propulsion Data. International Shipbuilding Progress.28:272-276.

Holtrop J. A statistical resistance prediction method with a speed dependent form factor. Proceedings of the Scientific and Methodological Seminar on Ship Hydrodynamics (SMSSH'88); 1988.

Holtrop J, Mennen G. 1982. An approximate power prediction method. International Shipbuilding Progress.29:166-170.

Ignizio JP. 1976. Goal Programming and Extensions: Lexington Books.

Kang L, Lu Z, Meng Q, Gao S, Wang F. 2019. Maritime simulator based determination of minimum DCPA and TCPA in head-on ship-to-ship collision avoidance in confined waters. Transportmetrica A: Transport Science. 2019/11/29;15:1124-1144.

Kuzu AC, Akyuz E, Arslan O. 2019. Application of Fuzzy Fault Tree Analysis (FFTA) to maritime industry: A risk analysing of ship mooring operation. Ocean Engineering. 2019/05/01/;179:128-134.

Leung SCH, Ng W-l. 2007. A goal programming model for production planning of perishable products with postponement. Computers & Industrial Engineering.53:531-541.

Liu Y, Zou L, Zou Z, Guo H. 2018. Predictions of ship maneuverability based on virtual captive model tests. Engineering Applications of Computational Fluid Mechanics. 2018/01/01;12:334-353.

Lu Z, Zao-jian Z, Yi L. 2019. CFD-based predictions of hydrodynamic forces in ship-tug boat interactions, Ships and Offshore Structures, 14:sup1, 300-310. 10.1080/17445302.2019.1589963.

Luo M, Shin S-H, Chang Y-T. 2017. Duration analysis for recurrent ship accidents. Maritime Policy & Management. 2017/07/04;44:603-622.

Moon DS-H, Woo JK. 2014. The impact of port operations on efficient ship operation from both economic and environmental perspectives. Maritime Policy & Management. 2014/07/29;41:444-461.

Nakamura S. 2017. Study on Manoeuvring Criteria for Safety Assessment in Shallow Water. TransNav, the International Journal on Marine Navigation and Safety of Sea Transportation.11:401-407.

Neri P. 2018. Time-domain simulator for short-term ship manoeuvring prediction: development and applications. Ships and Offshore Structures.14:249-264.

Papanikolaou A. 2014. Ship design: methodologies of preliminary design  Dordrecht, The Netherlands: Springer.

Paulauskas V, Simutis M, Plačiene B, Barzdžiukas R, Jonkus M, Paulauskas D. 2021. The Influence of Port Tugs on Improving the Navigational Safety of the Port. Journal of Marine Science and Engineering.9.

Pollalis C, Mourkogiannis D, Boulougouris E. 2021. Numerical simulation of a vessel's manoeuvring performance in regular waves. Ships and Offshore Structures.1-10.

Rameesha TV, Krishnankutty P. 2018. Numerical study on the manoeuvring of a container ship in regular waves. Ships and Offshore Structures.14:141-152.

Romero C. 2004. A general structure of achievement function for a goal programming model. European Journal of Operational Research. 2004/03/16/;153:675-686.

San Cristóbal JR. 2012b. A goal programming model for the optimal mix and location of renewable energy plants in the north of Spain. Renewable and Sustainable Energy Reviews. 2012/09/01/;16:4461-4464.

Seo M-G, Kim Y. 2011. Numerical analysis on ship maneuvering coupled with ship motion in waves. Ocean Engineering. 2011/12/01/;38:1934-1945.

Shahpanah A, Hashemi A, Nouredin G, Zahraee SM, Helmi SA. 2014. Reduction of Ship Waiting Time at Port Container Terminal Through Enhancement of the Tug/Pilot Machine Operation. Jurnal Teknologi. 05/01;68.

Shin S-H, Lee PT-W, Lee S-W. 2019. Lessons from bankruptcy of Hanjin Shipping Company in chartering. Maritime Policy & Management. 2019/02/17;46:136-155.

Tillig F, Ringsberg JW. 2018. A 4 DOF simulation model developed for fuel consumption prediction of ships at sea. Ships and Offshore Structures.14:112-120.

Ugurlu Ö, Yüksekyildiz E, Köse E. 2014. Simulation Model on Determining of Port Capacity and Queue Size: A Case Study for BOTAS Ceyhan Marine Terminal. TransNav, the International Journal on Marine Navigation and Safety of Sea Transportation.8:143-150.

URL-1, 2022. Available from https://msi.nga.mil/queryResults?publications/world-port-index?portName=GEMLIK&output=html

URL-2, 2021. Available from https://www.yilport.com/en/ports/gallery/Terminal-Layouts/296/517/0

Vantorre M, Eloot K, Delefortrie G, Lataire E, Candries M, Verwilligen J. 2017. Maneuvering in Shallow and Confined Water. In: Encyclopedia of Maritime and Offshore Engineering. p. 1-17.

Wang L-y, Tang Y-g, Li Y, Zhang J-c, Liu L-q. 2020. Studies on Stochastic Parametric Roll of Ship with Stochastic Averaging Method. China Ocean Engineering. 2020/04/01;34:289-298.

Wang T, Li G, Wu B, Æsøy V, Zhang H. 2021. Parameter identification of ship manoeuvring model under disturbance using support vector machine method. Ships and Offshore Structures.16:13-21.

Wang Z-y, Yu J-c, Zhang A-q, Wang Y-x, Zhao W-t. 2017. Parametric geometric model and hydrodynamic shape optimization of a flying-wing structure underwater glider. China Ocean Engineering. 2017/12/01;31:709-715.

Watson DG. 1998. Practical ship design  United Kingdom: Elsevier.

Xu H-f, Zou Z-j, Wu S-w, Liu X-y, Zou L. 2017. Bank effects on ship–ship hydrodynamic interaction in shallow water based on high-order panel method. Ships and Offshore Structures.12:843-861.

Xue J, Chen Z, Papadimitriou E, Wu C, Van Gelder PHAJM. 2019. Influence of environmental factors on human-like decision-making for intelligent ship. Ocean Engineering. 2019/08/15/;186:106060.

Yasukawa H, Yoshimura Y. 2015. Introduction of MMG standard method for ship maneuvering predictions. Journal of Marine Science and Technology. 2015/03/01;20:37-52.

Zinchenko S, Tovstokoryi O, Nosov P, Popovych I, Kyrychenko K. 2022. Pivot Point position determination and its use for manoeuvring a vessel, Ships and Offshore Structures. 10.1080/17445302.2022.2052480.

Zhang W, Zou Z-J, Deng D-H. 2017. A study on prediction of ship maneuvering in regular waves. Ocean Engineering.137:367-381.

Zheng J, Hou X, Qi J, Yang L. 2022. Liner ship scheduling with time-dependent port charges. Maritime Policy & Management. 2022/01/14;49:18-38.

# APPENDIXES

## Appendix I. Nomenclature.

| | | | |
|---|---|---|---|
| $A_{BT}$ | Transverse area of bulbous bow measured at forward perpendicular | $L_{PP}$ | Length between perpendiculars (m) |
| $B$ | The ship molded beam (m) | $L_R$ | Length of run (m) |
| $c_{FAh}$- $r_{FAh}$ | Ship headway coefficient under total resistance force and existing telegraph command (full ahead) | $L_{WL}$ | Length in waterline (m) |
| $C_{Cur}$ | Current speed co-efficient for ship environment | $M$ | Ship displacement (ton) |
| $C_T$ | Tugboat speed co-efficient | $m_1, m_3, m_4$ | Additional coefficients for the wave resistance |
| $C_B$ | Block co-efficient | $R_A$ | Model-ship correlation |
| $C_F$ | Model-ship correlation line co-efficient | $R_{AA}$ | Air resistance (N) |
| $C_M$ | Midship section coefficient | $R_{APP}$ | Appendage resistance (N) |
| $C_P$ | Prismatic coefficient | $R_B$ | Bulbous bow resistance (N) |
| $C_{stern}$ | A value for aft body shape | $R_F$ | Frictional resistance (N) |
| $C_{WP}$ | Waterplane area coefficient | $R_T$ | Total resistance (N) |
| $c_1$, $c_2$, $c_5$, $c_{17}$ | Coefficients for the wave resistance | $R_{TH}$ | The resistance of bow thruster tunnel opening |
| $c_6$ | Coefficient for transom resistance | $R_{TR}$ | Transom immersion resistance (N) |
| $c_{14}$ | A constant to evaluate the effect of the aft body shape. | $R_{Wa}$ | The wave resistance for Froude numbers $Fr < 0.4$ |
| $D$ | Exponent of the wave-making resistance | $R_{Wb}$ | The wave resistance for Froude numbers $Fr > 0.55$ |
| $Fr$ | Froude number | $S$ | Wetted surface ($m^2$) |
| $Fr_{design}$ | Design froude number | $S_{APP}$ | The wetted surface of appendages ($m^2$) |
| $Fr_i$ | Immersion froude number | $t_{AVG}$ | Average maneuvering time from starting point to berthing. |
| $G$ | Gravity ($m/s^2$) | $T$ | The molded mean draught |
| $h_B$ | Height of center of $A_{BT}$ above basis | $T_F$ | The molded draft at forward perpendicular |
| $h_F$ | Forward sinkage | $t_T$ | Tugboat operation time |
| $h_W$ | Local wave height | | |
| $i_E$ | Waterline entrance angle (°) | $\upsilon$ | Kinematic viscosity ($m^2/s$) |
| $K$ | Hull form factor | $\upsilon_S$ | Ship speed (m/s) |
| $k_2$ | Form factor for appendages | $\upsilon_{S1}, \upsilon_{S2}, \upsilon_{S3}$ | Ship speeds in time $t_1$, $t_2$ and $k_3$ |
| $k_3$ | Stopping constant for inertia | $P$ | Water density ($kg/m^3$) |
| $k_S$ | A standard value for surface roughness | $\rho_A$ | Air density ($kg/m^3$) |
| $L$ | Length (m) | $\lambda$ | Coefficient for the wave resistance |
| $LCB$ | Longitudinal center of buoyancy | $\nabla$ | Displacement Volume ($m^3$) |
| $COG$ | Course over ground | SOG | Speed over ground |

## Appendix II. Hydrodynamic Forces Through Ship Manoeuvring.

Total resistance equation ($R_T$) is defined such as Eq. A2.1 (Holtrop 1984):

$$R_T = (1+k)R_F + R_{APP} + R_W + R_B + R_{TR} + R_A + R_{AA} \tag{A2.1}$$

where, $k$ is a hull form factor which can be predicted by adapting the procedure as shown below (Birk 2019, Guldhammer and Harvald 1974, Holtrop 1977, Holtrop 1984):

$$k = -0.07 + 0.487118 c_{14} \left[ \left( \frac{B}{L_{WL}} \right)^{1.06806} \left( \frac{T}{L_{WL}} \right)^{0.46106} \left( \frac{L_{WL}}{L_R} \right)^{0.121563} \left( \frac{L_{WL}^3}{V} \right)^{0.36486} (1-C_P)^{-0.604247} \right] \tag{A2.2}$$

for,

$$c_{14} = 1.0 + 0.011 C_{stern}$$

$$L_R = L_{WL} \left( \frac{1 - C_P + 0.06 C_P LCB}{4C_P - 1} \right)$$

$$0.55 \le C_P \le 0.85$$

$$LCB = -\left(0.44 Fr_{\text{design}} - 0.094\right)$$

$$Fr = \frac{\upsilon_s}{\sqrt{g L_{WL}}} \le 0.45$$

$$3.9 \le \frac{L}{B} \le 9.5$$

In accordance with ITTC – 1957 model ship correlation line co-efficient, the formula of frictional resistance can be written on the basis of conceptual framework proposed by Holtrop and Mennen (1982), as shown below:

$$R_F = \frac{1}{2} \rho \upsilon_S^2 S C_F \tag{A2.3}$$

$$S = c_{23} L_{WL} (2T + B) \sqrt{C_M} + 2.38 \frac{A_{BT}}{C_B}$$

$$c_{23} = \left[ 0.453 + 0.4425 C_B - 0.2862 C_M - 0.003467 \frac{B}{T} + 0.3696 C_{WP} \right]$$

$$C_{B_{(\text{w.r.t } L_{WL})}} = \left( \frac{L_{PP}}{L_{WL}} \right) C_{B_{(\text{w.r.t } L_{PP})}}$$

In here, $C_M$ is estimated based on formula (A4) (Abel-Günther and Keil 1994) and $C_{WP}$ is a coefficient that can be calculated by considering the line plan of the ship (Bertram and Wobig 1999, Papanikolaou 2014, Watson 1998):

$$C_M = \frac{1}{1+\left(1-C_B\right)^{3.5}} \tag{A2.4}$$

$$C_{WP} = \begin{cases} 0.763\left(C_P + 0.34\right) & \text{for tanker, bulk carrier, general} \\ & \text{cargo with } 0.56 < C_P < 0.87 \\ 3.226\left(C_P - 0.36\right) & \text{for container ships with } 0.57 < C_P < 0.62 \end{cases} \tag{A2.5}$$

Holtrop (1988) and Birk (2019) investigated the differential impacts of ship appendages (rudders, shaft brackets, skeg, strut bossing, hull bossing, exposed shafts, stabilizer fins, dome, and bilge keels) on viscous resistance using experimental trials and formalized as Eq. A2.6:

$$R_{APP} = \frac{1}{2}\rho \upsilon_S^2 \left(1+k_2\right)_{\text{eq}} C_F \sum S_{APP} + \sum R_{TH} \tag{A2.6}$$

The wave resistance *($R_W$)* is defined with a function of Froude number (*Fr)* that may be computed with Eq. A7 (Birk 2019, Holtrop 1984) by considering positive impacts of bulbous bow and transom on the wave resistance (Holtrop 1988).

$$R_W = \begin{cases} R_{Wa}(Fr) = c_1 c_2 c_5 \rho g \nabla \exp\left[ m_1 Fr^d + m_4 \cos\left(\lambda Fr^{-2}\right)\right] & \text{if } Fr \le 0.4 \\ R_W(Fr) = R_{Wa}(0.4) + \dfrac{\left(20Fr-8\right)}{3}\left[R_{Wb}(0.55) - R_{Wa}(0.4)\right] & \text{if } 0.4 < Fr \le 0.55 \\ R_{Wb}(Fr) = c_{17} c_2 c_5 \rho g \nabla \exp\left[ m_3 Fr^d + m_4 \cos\left(\lambda Fr^{-2}\right)\right] & \text{if } 0.55 < Fr \end{cases} \tag{A2.7}$$

Surveys such as that conducted by Holtrop (1984) and Holtrop and Mennen (1982) have shown that the pressure resistance of bulbous bow ($R_B$) could be formulated as below:

$$R_B = 0.11\rho g \left(\sqrt{A_{BT}}\right)^3 \frac{Fr_i^3}{1+Fr_i^2} e^{\left(-3.0 P_B^{-2}\right)} \tag{A2.8}$$

$$Fr_i = \frac{\upsilon_S}{\sqrt{g\left(T_F - h_B - 0.25\sqrt{A_{BT}} + h_F + h_W\right)}}$$

$$h_F = C_P C_M \frac{BT}{L_{WL}}\left(136 - 316.3Fr\right)Fr^3 \quad \text{but } h_F \ge -0.01 L_{WL}$$

$$h_W = \frac{i_E \upsilon_S^2}{400g} \quad \text{but at most } h_W \le 0.01 L_{WL}$$

$$i_E = 1 + 89e^a$$

$$a = -\left[\left(\frac{L_{WL}}{B}\right)^{0.80856}\left(1-C_{WP}\right)^{0.30484}\left[1-C_P-0.0225LCB\right]^{0.6367}\left(\frac{L_R}{B}\right)^{0.34574}\left(\frac{100V}{L_{WL}^3}\right)^{0.16302}\right]$$

$$P_B = 0.56\frac{\sqrt{A_{BT}}}{T_F - 1.5h_B + h_F}$$

Similar to bulbous bow, a resistance force arises from an immersion transom in ship stern which is called transom resistance ($R_{TR}$). $R_{TR}$ is a function of a Froude number ($Fr_T$) which is expressed as below for $A_T$>0 transom area:

$$Fr_T = \frac{\upsilon_S}{\sqrt{\frac{2gA_T}{\left(B+BC_{WP}\right)}}} \tag{A2.9}$$

According to Birk (2019), the expression $A_T/\left(B+BC_{WP}\right)$ which is given in eq. A9, is used to measure the average draft of transom. If average draft is smaller than speed, the flow at the transom edge will become distinct and additional transom drag is zeroized. In this circumstance, $R_{TR}$ could be written as eq. A2.10.

$$R_{TR} = \frac{1}{2}\rho\upsilon_S^2 A_T c_6 \tag{A2.10}$$

$$c_6 = \begin{cases} 0.2(1-0.2Fr_T), \; for \ldots Fr_T < 5 \\ 0, \; for \ldots Fr_T > 5 \end{cases}$$

The correlation allowance coefficient and the additional coefficient are given as below (Holtrop and Mennen 1982) where $c_2$ is a coefficient which is defined in several studies (Birk 2019, Holtrop 1984):

$$R_A = \frac{1}{2}\rho\upsilon_S^2\left(C_A+\Delta C_A\right)\left[S+\sum S_{APP}\right] \tag{A2.11}$$

$$C_A = 0.00546\left(L_{WL}+100\right)^{-0.16} - 0.02 + 0.003\sqrt{\frac{L_{WL}}{7.5}}C_B^4 c_2\left(0.04-c_4\right)$$

$$c_4 = \begin{cases} \dfrac{T_F}{L_{WL}} & \text{if } T_F/L_{WL} \le 0.04 \\ 0.04 & \text{if } T_F/L_{WL} > 0.04 \end{cases}$$

$$\Delta C_A = \begin{cases} 0 & \text{if } k_S = 150\mu\text{m} \\ \dfrac{0.105k_S^{(1/3)} - 0.005579}{L_{WL}^{(1/3)}} & \text{if } k_S > 150\mu\text{m} \end{cases}$$

A ship can experience an additional force stemming from air flow in above the water line which is computed pertaining to the standard ITTC procedure (see, eq. A2.12).

$$R_{AA} = \frac{1}{2}\rho \upsilon_S^2 C_{DA} A_V \quad \text{(A2.12)}$$

where, $A_V$ is the area of the longitudinal projection of hull and superstructure above the waterline, $\rho_A = 1.225$ kg/m$^3$ is the density of air for standard atmospheric pressure and a temperature of 15 °C, and $C_{DA}$ = 0.8 is the default air drag coefficient.

Bertram (2012) uses the following equations to refer to ship inertia for a certain time (see, eq. A2.13) and distance (see, eq. A2.14) difference among two times or distances:

$$\Delta t = t_2 - t_1 = \frac{m}{k_3.\upsilon_{Sk_3}}\left[\arctan\frac{\upsilon_{S1}}{\upsilon_{Sk_3}} - \arctan\frac{\upsilon_{S2}}{\upsilon_{Sk_3}}\right] \quad \text{(A2.13)}$$

$$\Delta s = s_2 - s_1 = \frac{m}{2k_3}\ln\left(\frac{\upsilon_{S1}^2 + \upsilon_{Sk_3}^2}{\upsilon_{S2}^2 + \upsilon_{Sk_3}^2}\right) \quad \text{(A2.14)}$$

where,

$$m\upsilon_S^{'} = -k_3\left(\upsilon_S^2 + \upsilon_{Sk_3}^2\right), \upsilon_{Sk_3} = \upsilon_{S0}\sqrt{k_3/R_{T0}}, \frac{R_T}{\upsilon_S^2} = \frac{R_{T0}}{\upsilon_{S0}^2} = k_3$$

for 0 express values at beginning of the manoeuvring.

To be produced force by tugboats depends on tugboat horsepower (Paulauskas et al. 2021) and displacement amount ( $\Delta X$ ) of ships under the impact of tugboat pushing and pulling force ($F_{tug}$), ship inertia ($F_{inertia}$), total ship resistance force ($R_T$) and ship added mass ($m$) can be computed as follows for the tugboat planning process:

$$\Delta X = \frac{(F_{inertia} \mp F_{tug} - R_T).t^2}{2m} + V_0.t \quad \text{(A2.15)}$$

where $V_0$ is initial speed of ship and $t$ is time interval.

*Proof of Eq. A2.15:*

The Newton's second law defines the acceleration ( $\vec{a}$ ) with following formula:

$$\vec{a} = \frac{F_{net}}{m},$$

For the ship motion, $F_{net} = F_{inertia} \mp F_{tug} - R_T$,

Therefore, $\vec{a} = \frac{F_{net}}{m} = \frac{F_{inertia} \mp F_{tug} - R_T}{m}$

The acceleration of ship could be defined also with kinematic equation where it is

$$\Delta X = V_0.t + \frac{1}{2}\vec{a}t^2$$

In frame of Newton's second law and kinematic equation, acceleration of ship is

$$\frac{F_{inertia} \mp F_{tug} - R_T}{m} = \frac{2(\Delta X - V_0.t)}{t^2}$$

In here, displacement amount of ship could be written such as

$$\Delta X = \frac{(F_{inertia} \mp F_{tug} - R_T).t^2}{2m} + V_0.t$$

**Appendix III.** Details of the selected ships.

| | **Ship I** | **Ship II** |
|---|---|---|
| Ship type | Container | Container |
| Gross tonnage (GRT) | 17687 t | 40108 t |
| Deadweight ton (DWT) | 22028 t | 52806 t |
| Length overall (LOA) | 184.01 m | 257.88 m |
| Beam | 24.7 m | 32.25 m |
| Average service speed | 12.5 knots | 18.7 knots |
| Carrying capacity | 1604 TEU | 3900 TEU |
| Required tugboat number | 1 | 2 |
| Displacement (ton) | 36713.33 | 88010 |
| Scrubber | Available | Available |

644

**Appendix IV.** Ship I, Ship II and Tugboat Particulars.

| | Ship I | Ship II | Tugboat I | Tugboat II |
|---|---|---|---|---|
| Allocated tugboat | Tugboat I | Tugboat I & Tugboat II | - | - |
| Steering characteristics | | | | |
| • Steering device (type/no) | Becker's rudder/1 | Semi suspended/1 | Azimuth thruster/2 | Azimuth thruster/2 |
| • Maximum angle | 35 | 35 | 180 | 180 |
| • Number of bow thrusters | 1 | 1 | - | - |
| • Bow thrusters power | 1100 kW | 1600 kW | - | - |
| • Number of stern thrusters | 1 | - | - | - |
| • Stern thruster power | 600 kW | - | - | - |
| Stopping | | | | |
| • FAh to FAs | 354.6 s | 469.6 s | 12.9 s | 9.25 s |
| • HAh to HAs | 429.6 s | 478.6 s | 16.2 s | 10.25 s |
| • SAh to SAs | 610.6 s | 538.6 s | 19.2 s | 11.25 s |
| Main Engine(s) | | | | |
| • Type of main engine | Low speed diesel | Low speed diesel | High speed diesel | High speed diesel |
| • Number of main engine | 1 | 1 | 2 | 2 |
| • Maximum power per shaft | 1*11655 kW | 1*36540 kW | 2*1920 kW | 2*1566 kW |
| • Astern power | 60 % ahead | 32.84 % ahead | 100 % ahead | 100 % ahead |
| • Number of propellers | 1 | 1 | 2 | 2 |
| • Propeller rotation | Right | Right | Left/Right | Outward |
| • Min. RPM | 18 | 15 | 600 | 7 |
| • Emergency FAh to FAs | 66.4 s | 47.2 s | 9.8 s | 10.05 s |
| Engine Power (kW)/RPM per Engine Telegraph Order | | | | |
| • FAh | 4784/80 | 10355/66.5 | 1599/233.3 | 1189/246.8 |
| • HAh | 2185/60 | 5288/51 | 884/191.5 | 656/201.8 |
| • SAh | 768/40 | 3252/41 | 473/154.9 | 313/159.7 |
| • DSAh | 159/20 | 1805/30.5 | 217/118.4 | 106/109.8 |
| • DSAs | 193/-20 | 1652/-30.5 | - | - |
| • SAs | 1044/-40 | 3459/-41 | - | - |
| • HAs | 3115/-60 | 6145/-51 | - | - |
| • FAs | 6993/-80 | 12670/-66.5 | - | - |

645

**Appendix V.** Comparison of model results obtained by case study and measured data from real ship trial for Ship I.

| Measured data | | | | Model results | | | |
|---|---|---|---|---|---|---|---|
| Time (min) | COG | SOG (knot) | Engine Order | Time (min) | COG | SOG (knot) | Engine Order |
| **Course-keeping phase** | | | | | | | |
| t* | 172° | 3.4 | DSAh | t* | 172° | 4.1 | SAh |
| t+3 | 173° | 2.5 | SE | t+3 | 172° | 4.8 | HAh |
| t+6 | 172° | 2 | SE | t+6 | 172° | 5.7 | SE |
| t+9 | 172° | 1.2 | DSAh | t+9 | 172° | 2.5 | DSAh |
| **Course-altering phase** | | | | | | | |
| t+12 | 171° | 2.4 | SAh | t+11 | 156° | 3.9 | SAh |
| t+15 | 166° | 4.1 | DSAh | t+13 | 142° | 5.2 | HAh |
| t+17 | 163° | 3.7 | DSAh | t+15 | 122° | 4.5 | SAh |
| t+19 | 150° | 2.5 | SE | | | | |
| t+22 | 139° | 1.5 | SE | | | | |
| **Speed-reducing phase** | | | | | | | |
| t+25 | 139° | 1.1 | SE | t+16 | 122° | 3 | DSAh |
| | | | | t+16.27 | 122° | 2.8 | SE |
| | | | | Tugboat in pulling position | | | |
| | | | | t+17.09 | 122° | 0.7 | SE |
| | | | | End of pulling & start pushing operation by tugboat | | | |
| **Lateral shifting phase with tugboat pushing support** | | | | | | | |
| t+29 | 092° | 0.7 | SE | t+25 | 089° | 0.5 | SE |
| t+32 | 069° | 0 | SE | t+27.36 | 069° | 0 | SE |

*t is the starting time of maneuvering

**Appendix VI.** Comparison of model results obtained by case study and measured data from real ship trial for Ship II.

| Measured data | | | | Model results | | | |
|---|---|---|---|---|---|---|---|
| Time (min) | COG | SOG | Engine Order | Time (min) | COG | SOG | Engine Order |
| **Course-keeping phase** | | | | | | | |
| t* | 089° | 2.4 | DSAh | t* | 089° | 2.4 | DSAh |
| t+7 | 089° | 3.6 | Sah | t+2 | 090° | 3.1 | SAh |
| t+11 | 090° | 5.7 | Hah | t+5 | 090° | 4.6 | HAh |
| t+13 | 089° | 6.8 | Hah | t+23.5 | 090° | 7.6 | HAh |
| t+17 | 089° | 7.5 | Hah | t+26 | 090° | 5 | SAh |
| t+19 | 089° | 7.7 | Hah | | | | |
| t+22 | 090° | 7.8 | Hah | | | | |
| t+24 | 090° | 7.8 | Hah | | | | |
| t+27 | 090° | 7.8 | Sah | | | | |
| t+29 | 089° | 5.9 | Sah | | | | |
| t+32 | 089° | 4.6 | Hah | | | | |
| **Course-altering phase** | | | | | | | |
| t+35 | 112° | 5.1 | Hah | t+30 | 110° | 4.2 | DSAh |
| t+37 | 122° | 5.9 | Hah | t+32 | 120° | 2 | DSAh |
| t+39 | 146° | 5.9 | Sah | t+34 | 150° | 0.8 | SE |
| t+42 | 150° | 4.5 | DSAh | Tugboat in pushing position | | | |
| | | | | t+35.5 | 120° | 0.8 | SE |
| | | | | t+37.6 | 090° | 0.8 | DSAh |
| | | | | t+38.63 | 080° | 2.4 | HAh |
| | | | | End of pushing operation | | | |
| **Speed-reducing phase** | | | | | | | |
| t+44 | 150° | 3.7 | DSAh | t+41 | 080° | 4.2 | DSAh |
| t+47 | 150° | 2.1 | SE | t+43 | 080° | 2.2 | SE |
| t+51 | 150° | 0.8 | SE | Tugboat in pulling position | | | |
| | | | | t+43.13 | 079° | 0.4 | SE |
| | | | | End of pulling & start of pushing operation | | | |
| **Lateral shifting phase with tugboat pushing support** | | | | | | | |
| t+54 | 110° | 0.5 | SE | t+46 | 062° | 0.3 | SE |
| t+57 | 076° | 0.3 | SE | t+48.05 | 044° | 0 | SE |
| t+61 | 044° | 0 | SE | | | | |

*t is the starting time of manoeuvring.

**Appendix VII.** Onboard Manoeuvring Trial Results for Determining Speed Reduction in Straight Line for Different Telegraph Command.

| | **Ship I** | **Ship II** |
|---|---|---|
| FAh to Hah | 46 s | 58 s |
| HAh to Sah | 69 s | 78 s |
| SAh to DSAh | 139 s | 216 s |
| DSAh to SE | 774 s | 940 s |

**Appendix VIII.** Calculated resistance forces for Ship I and Ship II.

| | SOG (kn) | Reynolds Number | $Fr$ | $R_F$ | $R_{TH}$ | $R_{APP}$ | $R_W$ | $R_B$ | $R_{TR}$ | $R_A$ | $R_{AA}$ | $R_T$ |
|---|---|---|---|---|---|---|---|---|---|---|---|---|
| *Ship I* | 4.08 | 3.1342E+08 | 0.050 | 36771.747 | 46.202 | 248.700331 | 0.000 | 1.2651E-03 | 1.1419E+03 | 4113.92591 | 0 | 4.2322E+04 |
| | 5.84 | 4.4884E+08 | 0.072 | 70266.069 | 94.752 | 475.234277 | 1.29E+00 | 3.4760E-03 | 1.8134E+03 | 8436.99356 | 0 | 81087.76751 |
| | 4.87 | 3.7429E+08 | 0.060 | 46184.047 | 65.890 | 312.359042 | 3.17E-02 | 2.0586E-03 | 1.4633E+03 | 5867.05211 | 0 | 53892.72932 |
| | 2.38 | 1.8292E+08 | 0.029 | 10872.682 | 15.737 | 73.5357935 | 7.13E-12 | 2.5460E-04 | 4.7352E+02 | 1401.25101 | 0 | 12836.72871 |
| *Ship II* | 2.38 | 255787606.1 | 0.0247979 | 23554.73664 | 15.7368806 | 84.7102249 | 2.715E-14 | 2.6177E-04 | 456.0593943 | 1835.13694 | 0 | 25946.38034 |
| | 7.58 | 814651283.1 | 0.0789782 | 238925.6356 | 159.625822 | 859.251565 | 21.106122 | 2.6177E-04 | 4626.002928 | 18614.5685 | 0 | 263206.1909 |
| | 4.97 | 534144706.8 | 0.0517839 | 102715.7677 | 68.6242344 | 369.398135 | 0.00378 | 2.6177E-04 | 1988.750352 | 8002.53055 | 0 | 113145.075 |
| | 4.17 | 448165679.5 | 0.0434484 | 72309.68151 | 48.3099786 | 260.048307 | 3.54E-05 | 2.6177E-04 | 1400.037286 | 5633.60863 | 0 | 79651.68602 |
| | 2.03 | 218171781.6 | 0.0211512 | 17136.27467 | 11.4487168 | 61.6274214 | 7.832E-18 | 2.6177E-04 | 331.7871545 | 1335.078 | 0 | 18876.21622 |
| | 0.77 | 82754813.72 | 0.0080229 | 2465.504441 | 1.64719944 | 8.86672769 | 8.531E-55 | 2.6177E-04 | 47.73632069 | 192.086133 | 0 | 2715.841083 |
| | 0.77 | 82754813.72 | 0.0080229 | 2465.504441 | 1.64719944 | 8.86672769 | 8.531E-55 | 2.6177E-04 | 47.73632069 | 192.086133 | 0 | 2715.841083 |
| | 0.77 | 82754813.72 | 0.0080229 | 2465.504441 | 1.64719944 | 8.86672769 | 8.531E-55 | 2.6177E-04 | 47.73632069 | 192.086133 | 0 | 2715.841083 |
| | 2.38 | 255787606.1 | 0.0247979 | 23554.73664 | 15.7368806 | 84.7102249 | 2.715E-14 | 2.6177E-04 | 456.0593943 | 1835.13694 | 0 | 25946.38034 |
| | 4.17 | 448165679.5 | 0.0434484 | 72309.68151 | 48.3099786 | 260.048307 | 3.54E-05 | 2.6177E-04 | 1400.037286 | 5633.60863 | 0 | 79651.68602 |